Contents lists available at ScienceDirect

Biosensors and Bioelectronics

journal homepage: http://ees.elsevier.com

Competitive upconversion-linked immunoassay using peptide mimetics for the detection of the mycotoxin zearalenone

Riikka Peltomaa [a,b,1], Zdeněk Farka [a,c], Matthias J. Mickert [a,2], Julian C. Brandmeier [a], Matěj Pastucha [c], Antonín Hlaváček [d], Mónica Martínez-Orts [e], Ángeles Canales [e], Petr Skládal [c], Elena Benito-Peña [b], María C. Moreno-Bondi [b,**], Hans H. Gorris [a,*]

[a] Institute of Analytical Chemistry, Chemo- and Biosensors, University of Regensburg, Universitätsstraße 31, 93040, Regensburg, Germany
[b] Department of Analytical Chemistry, Faculty of Chemistry, Universidad Complutense de Madrid, Plaza de las Ciencias, Ciudad Universitaria, 28040, Madrid, Spain
[c] Department of Biochemistry, Faculty of Science, Masaryk University, Kamenice 5, 625 00, Brno, Czech Republic
[d] Institute of Analytical Chemistry of the Czech Academy of Sciences, Veveří 97, 602 00, Brno, Czech Republic
[e] Department of Organic Chemistry, Faculty of Chemistry, Universidad Complutense de Madrid, Plaza de las Ciencias, Ciudad Universitaria, 28040, Madrid, Spain

ARTICLE INFO

Keywords
Zearalenone
Upconversion nanoparticle
Peptide mimetic
Immunosensing
Surface plasmon resonance
Food safety

ABSTRACT

Due to increasing food safety standards, the analysis of mycotoxins has become essential in the food industry. In this work, we have developed a competitive upconversion-linked immunosorbent assay (ULISA) for the analysis of zearalenone (ZEA), one of the most frequently encountered mycotoxins in food worldwide. Instead of a toxin-conjugate conventionally used in competitive immunoassays, we designed a ZEA mimicking peptide extended by a biotin-linker and confirmed its excellent suitability to mimic ZEA by nuclear magnetic resonance (NMR) and surface plasmon resonance (SPR) analysis. Upconversion nanoparticles (UCNP, type $NaYF_4$:Yb,Tm) served as background-free optical label for the detection of the peptide mimetic in the competitive ULISA. Streptavidin-conjugated UCNPs were prepared by click reaction using an alkyne-PEG-neridronate linker. The UCNP conjugate clearly outperformed conventional labels such as enzymes or fluorescent dyes. With a limit of detection of 20 pg mL^{-1} (63 pM), the competitive ULISA is well applicable to the detection of ZEA at the levels set by the European legislation. Moreover, the ULISA is specific for ZEA and its metabolites (α- and β-zearalenol) without significant cross-reactivity with other related mycotoxins. We detected ZEA in spiked and naturally contaminated maize samples using liquid chromatography–tandem mass spectrometry (UPLC-MS/MS) as a reference method to demonstrate food analysis in real samples.

1. Introduction

Zearalenone (ZEA) is a non-steroidal estrogenic mycotoxin that is produced as a secondary metabolite by several fungi species in the *Fusarium* genus (Bennett and Klich, 2003; Zinedine et al., 2007). Although ZEA is acknowledged to exhibit relatively low acute toxicity, it is chronically toxic and has been frequently implicated in reproductive disorders of farm animals, especially pigs (Kuiper-Goodman et al., 1987; Zinedine et al., 2007). Estrogenic activity accounts for its most critical mode of action, although ZEA has also been implicated in anabolic, haematotoxic, and genotoxic effects (Kuiper-Goodman et al., 1987; IARC, 1993; Maaroufi et al., 1996; European Commission, 2000). Alongside with other mycotoxins, ZEA is a common contaminant in many agricultural commodities, such as maize, barley, oats, wheat, and rice (EFSA Panel, 2011). Maize and maize-based products are the most frequently contaminated food commodities. As much as 79% of tested samples have been reported to be contaminated with ZEA at detectable levels (Gareis et al., 2003). Due to their widespread and extensive biological effects, current international and national regulations encompass ZEA and other major mycotoxins (van Egmond et al., 2007). Current maximum limits for ZEA in Europe vary from 20 to 3000 μg kg^{-1} depending on the foodstuffs or animal feed in question (European Commission, 2006a, 2006b). The legislation inevitably calls for sensitive and accurate analytical methods to detect the toxins and to ensure safe food for the consumer.

* Corresponding author.
** Corresponding author.
E-mail addresses: mcmbondi@ucm.es (M.C. Moreno-Bondi); hans-heiner.gorris@ur.de (H.H. Gorris)
[1] Department of Biochemistry/Biotechnology, University of Turku, Kiinamyllynkatu 10, 20520, Turku, Finland.
[2] Lumito AB, Gasverksgatan 1, SE-222 29 Lund, Sweden.

https://doi.org/10.1016/j.bios.2020.112683
Received 6 August 2020; Received in revised form 18 September 2020; Accepted 2 October 2020
Available online xxx
0956-5663/

High-performance liquid chromatography (HPLC) coupled with fluorescence (De Saeger et al., 2003; Drzymala et al., 2015) or mass spectrometry (Romera et al., 2018; Hidalgo-Ruiz et al., 2019) detectors are commonly used as reference methods for the detection of ZEA. Besides these sensitive yet complex and costly chromatographic techniques, immunochemical methods such as enzyme-linked immunosorbent assays (ELISAs) are fast and straightforward screening techniques for on-site mycotoxin analysis (EFSA Panel, 2011; Nolan et al., 2019; Caglayan et al., 2020). Small molecules such as ZEA are conventionally detected in a competitive ELISA format, which, however, suffers from certain inherent limitations (Wild, 2013; Nolan et al., 2019). The synthesis of competing mycotoxin-conjugates accounts for one of the main challenges (Xiong et al., 2020). For instance, ZEA has no suitable reactive groups available for coupling such that the conjugation to a carrier protein or a label requires large amounts of the pure toxin, involves several reaction steps that may result in a heterogeneous mixture of conjugates with different stoichiometries and a challenging purification (Liu et al., 1985; Thouvenot and Morfin, 1983). Large batch-to-batch variations and overuse of organic solvents in the conjugation account for additional limitations. There is also a potential toxicity hazard for the manufacturer, user, and the environment (Chauhan et al., 2016).

Epitope mimicking peptides, also known as mimotopes, have been introduced as a valuable alternative to the traditional analyte-conjugates in competitive immunoassays and biosensors. Such peptides mimic the epitope of the analyte sufficiently to compete with the native analyte for antibody binding. Therefore, the cumbersome conjugation step and the aforementioned limitations can be avoided (Xiong et al., 2020; Peltomaa et al., 2018a). It should also be noted that although high-affinity antibodies are of crucial importance for high sensitivity in all immunoassays, a lower affinity of the peptide competitor compared to the analyte shifts the equilibrium in favor of analyte binding (Peltomaa et al., 2019; Xiong et al., 2020). As less analyte is required to achieve the same response, the assay is more sensitive. Peptide mimetics for many mycotoxins have been identified from peptide libraries by phage display (Yuan et al., 1999; He et al., 2011, 2013; Liu et al., 2013; Peltomaa et al., 2017). From such a phage-borne peptide mimetic for ZEA, we have previously constructed a recombinant peptidomimetic fusion protein with *Gaussia* luciferase. This bioluminescent tracer was directly used for the detection of ZEA without the need for secondary antibodies or further labeling steps and achieved a limit of detection (LOD) of 4.2 ng mL^{-1} (Peltomaa et al., 2020).

The progress in nanotechnology-based biosensors (Farka et al., 2017) has also inspired the field of mycotoxin detection. Several nanoparticles (NP) have been used as the detection label, for example, lanthanide-doped inorganic NPs (Niazi et al., 2018), gold (Peltomaa et al., 2018b; Liu et al., 2020) and silver NPs (Jiang et al., 2020), quantum dots (Fang et al., 2014; Li et al., 2019), silica NPs (Taghdisi et al., 2016; Tan et al., 2019) as well as photon-upconversion nanoparticles (UCNP) (Dai et al., 2017; Wu et al., 2018; Yang et al., 2018; He et al., 2020). UCNPs are lanthanide-doped nanomaterials capable of converting near-infrared (NIR) excitation light to emission at shorter wavelengths, typically in the visible range. The upconversion—or anti-Stokes—emission can be detected without optical background interference or light scattering, and the autofluorescence is completely eliminated by spectral separation (Haase and Schäfer, 2011). Owing to these unique optical properties, UCNPs have gained significant attention and become an intriguing alternative for enzymatic or fluorescent labels in immunoassays (Hlaváček et al., 2016; Farka et al., 2020a), lateral flow assays (Sedlmeier et al., 2016; Zhang et al., 2020) as well as biosensors (Farka et al., 2017; Zhang et al., 2019; Kim et al., 2020).

To account for the growing need for the rapid analysis of ZEA, we introduce a highly sensitive competitive upconversion-linked immunosorbent assay (ULISA) for the detection of ZEA based on a synthetic peptide mimetic and UCNPs as the label. As shown schematically in Fig. 1, our approach relies on the use of the previously identified ZEA mimicking peptide (Peltomaa et al., 2020), which was chemically synthesized and modified with a biotin linker, and thoroughly characterized. To the best of our knowledge, we have analyzed for the first time both the interaction of peptide mimetic and antibody by nuclear magnetic resonance (NMR) and its binding kinetics by surface plasmon resonance (SPR). We functionalized UCNPs with a PEG-linker and streptavidin (UCNP-PEG-SA) as a highly sensitive label for ZEA detection. After confirming the specificity of the method in cross-reactivity studies, spiked and naturally contaminated maize samples were analyzed.

2. Experimental section

2.1. Materials

Monoclonal anti-zearalenone (anti-ZEA) antibody was purchased from Soft Flow Ltd (Pécs, Hungary). The biotinylated peptide mimetic (GWWGPYGEIELLGGGSK(Bio)-NH_2) was synthesized at Peptide Synthetics (Fareham, UK). Mycotoxins zearalenone (ZEA), α-zearalenol, and β-zearalenol were supplied by Sigma-Aldrich (St. Louis, MO, USA), whereas fumonisin B_1, deoxynivalenol, T-2 toxin, and ochratoxin A were from Fermentek Ltd. (Jerusalem, Israel). Human serum albumin-conjugated ZEA (HSA-ZEA) was from BioTez (Berlin, Germany). SuperBlock (TBS) Blocking Buffer was purchased from Thermo Fisher Scientific (Waltham, MA, USA), bovine γ-globulin (BGG), bovine serum albumin (BSA), and Tween-20 were purchased from Sigma-Aldrich. The 96-well microtiter plates with a clear bottom (μClear, high binding) were obtained from Greiner Bio-One (Kremsmünster, Austria). The preparation, surface conjugation, and characterization of UCNPs are described in the supporting information (SI).

2.2. Peptide characterization by NMR spectroscopy and SPR analysis

Saturation transfer difference (STD) experiments were performed using a Bruker AVANCE 600 MHz spectrometer equipped with a cryogenic probe, with 4096 scans, at 298 K. The irradiation conditions were set at −1.0 ppm for the on-resonance and 100 ppm for the off-resonance spectra, respectively. Samples were dissolved in deuterated PBS buffer to a final concentration of 0.4 mM for the peptide mimetic and 3 μM for the anti-ZEA antibody. For the competitive binding experiment, ZEA was added to the peptide/antibody sample to a final concentration of 0.2 mM (peptide–toxin ratio 2:1). The binding kinetics of the peptide mimetic was studied on an MP-SPR Navi 210 A (BioNavis, Finland) SPR system. Details of the affinity measurements can be found in the SI.

2.3. Competitive immunoassays

The ELISA and fluorescent immunoassay (FIA) are described in the SI. For the ULISA, a 96-well microtiter plate was coated with 2 μg mL^{-1} of anti-ZEA monoclonal antibody in coating buffer (50 mM $NaHCO_3/Na_2CO_3$, pH 9.6, supplemented with 0.05% (w/v) NaN_3; 100 μL per well) by overnight incubation at 4 °C. After washing the wells four times with washing buffer (50 mM Tris, pH 7.5; 0.05% (w/v) Tween 20, 0.05% (w/v) NaN_3) using a plate washer (HydroFlex, Tecan, Switzerland), they were blocked with 175 μL of blocking buffer (50 mM Tris-HCl, pH 7.4; 10% (v/v) SuperBlock, 0.05% (w/v) NaN_3; 150 mM NaCl) for 1 h at room temperature. After repeating the washing steps, standard dilutions of ZEA in the range of 0–100 ng mL^{-1} were added to the wells in triplicates together with the peptide mimetic (2 μg mL^{-1}) in a total volume of 100 μL per well in assay buffer (50 mM Tris-HCl, pH 7.5; 150 mM NaCl, 0.05% (w/v) NaN_3, 0.01%

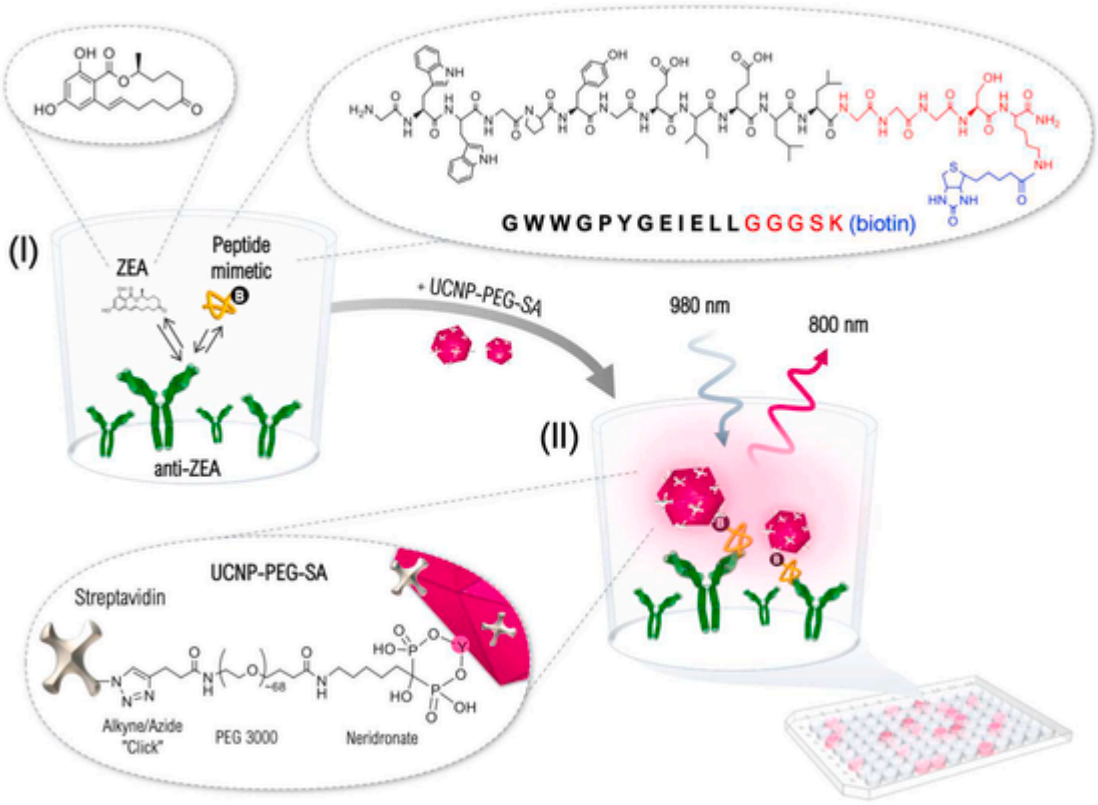

Fig. 1. Scheme of the competitive ULISA for the detection of zearalenone (ZEA). In the first step (I), a microtiter plate is coated with anti-ZEA antibody, and ZEA in the sample competes with the peptide mimetic for a limited amount of antibody binding sites. The peptide of 12 amino acids was extended by a GGGSK-linker (red) on the C-terminus including biotin (blue) for coupling. In the second step (II), the UCNP-PEG-SA-conjugates bind to the biotinylated peptide, and high upconversion luminescence signals are measured in the absence of ZEA. Streptavidin is bound to the surface of UCNPs by using a PEG-neridronate linker (bottom left). (For interpretation of the references to color in this figure legend, the reader is referred to the Web version of this article.)

(w/v) Tween 20, 0.5% (w/v) BGG, 0.2% (w/v) BSA, 0.2% (v/w) poly(vinyl alcohol) 6000, 1% (w/v) glucose, 5 mM ethylenediaminetetraacetic acid). For the cross-reactivity study, ZEA was replaced by other mycotoxins. The incubation was continued for another 1 h, and after washing the wells four times, the UCNP-PEG-SA-conjugate (12.5 μg mL^{-1} in assay buffer) was added to each well. After 1 h of incubation and four washing steps, the plate was dried, and the upconversion luminescence was measured using a microtiter plate reader (Chameleon, Hidex, Finland) (Sedlmeier et al., 2016). In each well, 64 points were raster-scanned using a step size of 1 mm and a signal integration time of 1 s.

2.4. Analysis of real samples

Maize samples were provided by an external laboratory in Madrid (Spain), and the concentration of ZEA in the samples was determined by ultra-performance liquid chromatography–tandem mass spectrometry (UPLC-MS/MS) (Romera et al., 2018). For validation purposes and following current legislation (Magnusson and Örnemark, 2014), blank maize samples (1 g) that did not contain ZEA at levels detectable by UHPLC-MS/MS were spiked to 20–80 μg kg^{-1} of ZEA by adding a standard ZEA solution in methanol. After allowing the spiked samples to equilibrate overnight at room temperature, 5 mL of methanol:water mixture (80:20, v/v) was added, and the suspensions were shaken for 30 min at room temperature. Similarly, 5 mL of the solvent was added to 1 g of naturally contaminated maize samples that were also analyzed by UPLC-MS/MS according to a previously reported method (Romera et al., 2018). The sample extracts were purified by centrifugation (7000 × *g*, 10 min). Finally, the extracts were diluted 10 or 20 times in the assay buffer for the ULISA analysis.

2.5. Data analysis

The truncated average of the 64 measurement points was calculated for each well after discarding the 16 highest and 16 lowest measurements to account for irregularities in the luminescence readout of the well surface. The average luminescence signals obtained for different toxin concentrations were then analyzed with the data analysis and graphing software Origin (OriginLab, USA) using a four-parameter logistic regression model:

$$y = A_{min} + \frac{A_{max} - A_{min}}{1 + \left(\frac{x}{IC_{50}}\right)^{b}} \quad (1)$$

where A_{max} is the asymptotic maximum (*i.e.,* the signal in the absence of analyte), A_{min} is the asymptotic minimum, and b and IC_{50} are the slope of the curve and the analyte concentration at the inflection point, respectively.

The limit of detection (LOD) was determined as the toxin concentration at which the antibody binding to the peptide was inhibited by 10%, and the dynamic range was evaluated as the toxin concentration corresponding to 20–80% inhibition (Marco et al., 1995). Cross-reactivity (CR) was calculated from the IC_{50} values using the equation:

$$CR = \frac{IC_{50}\,(ZEA)}{IC_{50}\,(other\ \ mycotoxins)} \times 100\% \quad (2)$$

The apparent recovery from each spiked sample was calculated as the ratio of observed toxin concentration and the reference value.

3. Results and discussion

3.1. Design of the peptide mimetic for the competition with ZEA

The rapid analysis of low-molecular weight analytes such as zearalenone (ZEA) using competitive immunoassays poses particular challenges. These intrinsic limitations can be partially avoided by epitope mimicking peptides. A ZEA mimicking peptide (peptide mimetic) was identified by phage display without prior knowledge of the interaction between the antibody and ZEA. The selectivity of the peptide mimetic was ensured during the phage display selections using a competitive elution step with the target analyte in the panning process. Only those phages that displayed peptides capable of competing with ZEA were selected for the next round in the iterative panning process. A thorough selectivity study with the identified peptide mimetic showed that it interacted only with the anti-ZEA antibody and that it could be only displaced by ZEA and not by other mycotoxins (Peltomaa et al., 2020). In this work, we extended the C-terminus of the previously identified peptide mimetic by a short GGGSK(biotin) sequence as shown in Fig. 1 to (1) obtain a similar structure as the recombinant fusion and phage-displayed peptides, and (2) to introduce a biotin handle for the immobilization of the peptide to a solid surface or to a label via streptavidin. Moreover, in order to mimic the structure of the phage-displayed peptide as closely as possible, the C-terminus of the synthetic peptide was amidated to mask the negatively charged carboxylate group that was not present in the phage during the panning selections.

3.2. Analysis of the peptide–antibody interaction by NMR

To identify the key amino acids in the peptide mimetic (Fig. 1; top right inset) that contribute to the antibody binding, we studied the peptide–antibody interaction by NMR. The interaction between the peptide mimetic and anti-ZEA antibody was assessed using saturation transfer difference (STD) experiments, which are based on the magnetization transfer from a protein to the hydrogens of a bound ligand. When the resonances of the protein, here the anti-ZEA antibody, are selectively saturated, the signals of a specifically bound peptide show changes in the resonance intensity, and these signals can be detected in the STD. As the STD is the difference spectrum between the experiment with protein saturation and the reference spectrum without saturation, those signals that are not involved in the interaction are canceled in the STD (Mayer and Meyer, 1999). Clear STD signals were detected from the peptide mimetic in the presence of anti-ZEA, showing that the peptide is recognized by the antibody (Fig. 2A, the 2D experiments acquired for the aromatic signal assignment are given in Figs. S1–S2). In addition, STD intensities provided information about the binding epitope since the peptide regions that are more strongly involved in the interaction display higher STD values. Here, high STD values were detected

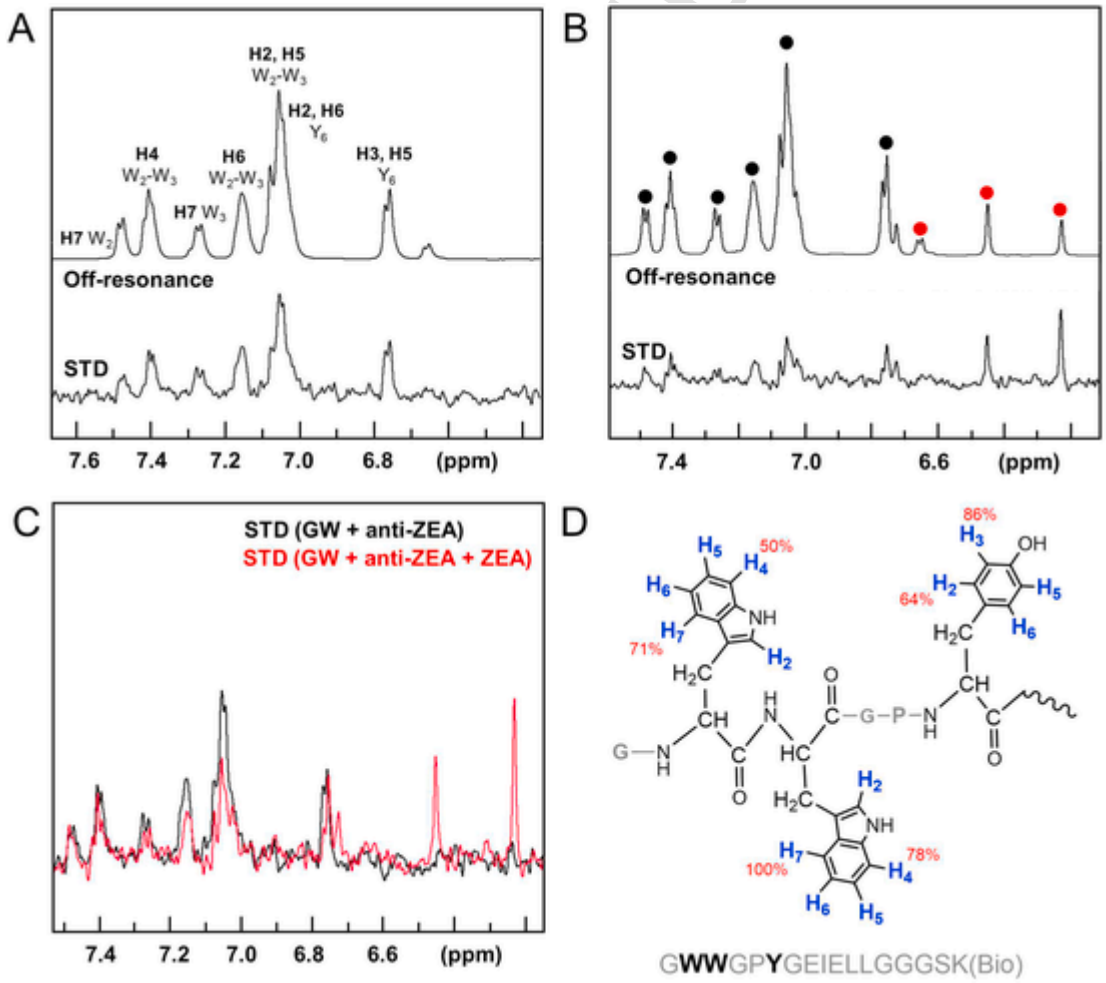

Fig. 2. Analysis of peptide–antibody interaction by STD-NMR experiments. Expansion of the aromatic region of the ^{1}H-NMR reference spectra (off-resonance) and STD spectra of the peptide mimetic in the presence of the anti-ZEA antibody (A) before and (B) after the addition of ZEA. The new peaks appearing in (B) are marked with red circles. (C) Overlay of STD spectra shown in panels (A) and (B). (D) Peptide regions that strongly interact with the antibody expressed as STD percentages of the differential spectrum normalized to H_7 of tryptophan 3 (W_3), which shows the highest STD value (100%). (For interpretation of the references to color in this figure legend, the reader is referred to the Web version of this article.)

for the aromatic residues tryptophan 2 and 3, and tyrosine 6. Tryptophan 3 was the residue with the highest STD effect (Fig. 2D). These results indicate that the aromatic amino acids of the peptide mimetic are the key interaction points with the antibody. This information can be of help for redesigning the peptide mimetic, for example, to a shorter format which could be more convenient and cost-effective for future studies. As a control experiment, the STD spectrum of the peptide was acquired in the absence of the antibody to check that no signals were detectable under these conditions (Fig. S3). Additionally, competitive binding experiments were performed by adding ZEA to the peptide/antibody sample and acquiring a new STD spectrum. As expected, we observed the signals of ZEA and a decrease of the peptide STD signals (Fig. 2B and C). This effect has been quantified by the measurement of the STD intensities in presence of 0.5 equivalents of ZEA. Under these conditions, the STD effect of the H7 signal from the tryptophan 3 (which is the most representative nucleus involved in the interaction) shows a decrease of 43% upon toxin addition. Simultaneously, the signals corresponding to ZEA display the highest STD effects (with intensities almost three times greater than the STD of the peptide signals). This confirms that both molecules—the peptide and the toxin—are competing for the same antibody binding site, and the interaction is specific.

3.3. Analysis of the peptide-binding kinetics by SPR

The binding kinetics of both the peptide mimetic and ZEA with the anti-ZEA antibody were evaluated and compared by SPR analysis (Fig. 3). For the investigation of the peptide mimetic (MW: 2031 g mol^{-1}), the antibody was immobilized on the chip, and the peptide mimetic was present in solution (Fig. 3A). Both fitting this kinetic data (one-to-one binding model) and a Langmuir equilibrium fit (Fig. S4) resulted in similar equilibrium constants (K_D) of 5.2×10^{-7} M or 2.2×10^{-7}, respectively. A similar K_D of 1.7×10^{-7} M was also found for a fumonisin mimetic peptide selected from the same phage-displayed peptide library in a previous study (Peltomaa et al., 2019).

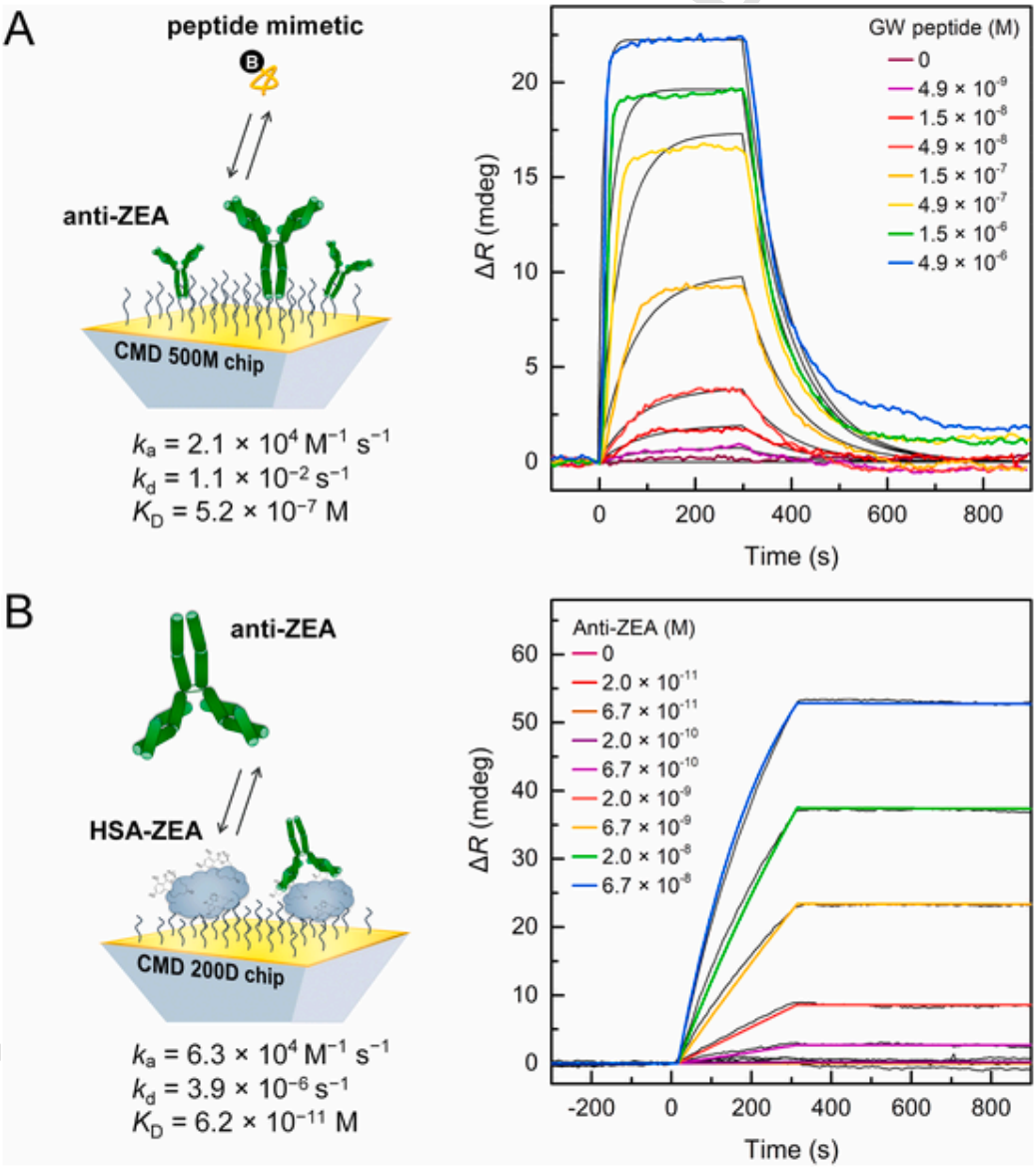

Fig. 3. Kinetic analyses by SPR using (A) the immobilized anti-ZEA antibody and free peptide mimetic, or (B) anti-ZEA antibody with immobilized HSA-ZEA. Binding curves with different peptide or antibody concentrations in colors are shown together with the kinetic fits in black. The differential signals Δ*R* were calculated from the sample and reference channels. (For interpretation of the references to color in this figure legend, the reader is referred to the Web version of this article.)

However, due to the small size of ZEA (MW: 318 g mol^{-1}), it was not possible to investigate the binding kinetics of ZEA in the same direct assay based on the immobilized antibody (data not shown). Therefore, an HSA-ZEA conjugate was immobilized on the SPR chip to capture the antibody in solution (Fig. 3B). In this case, K_D for the interaction of antibody and ZEA was much higher compared to the antibody–peptide interaction. While the association rates (k_a) are quite similar, the 10,000-fold faster dissociation rate (k_d) of the antibody-peptide complex account for the overall low K_D. Since each HSA molecule was conjugated on average to 12 ZEA molecules according to the manufacturer, both binding sites of the antibody may have been involved in binding to the HSA-ZEA conjugate, thus giving information on the stronger avidity rather than affinity. Nevertheless, these results show that the peptide mimetic binds less strongly to the antibody than ZEA, which renders the peptide a suitable competitor for the development of immunoassays.

3.4. Competitive ELISA and FIA

Conventional ELISA and fluorescence-linked immunoassay (FIA) are commonly used bioanalytical methods for mycotoxin analysis. In order to find the optimal label for the detection of ZEA using the synthetic peptide mimetic, we performed the assay with streptavidin conjugated either to horseradish peroxidase (SA-HRP) or carboxyfluorescein (SA-FAM). The functionality of both streptavidin labels was first confirmed by a binding study in a BSA-biotin assay. Relatively high BSA-biotin coating concentrations (10 μg mL^{-1}) were required for the reliable detection of the labels (Fig. S5) and resulted in signal-to-background ratios (S/B) of 69 for SA-HRP and 39 for SA-FAM.

In the competitive assay, using a capture antibody concentration of 2 μg mL^{-1}, the signal decreased slightly in response to increasing ZEA concentrations (Figs. S6A and S6B). Neither SA-HRP nor SA-FAM, however, were suitable to determine ZEA concentrations reliably. The insufficient label performance can be explained by the lower affinity of the peptide mimetic to the antibody as compared to ZEA (Fig. 3). While the lower affinity has the advantage that ZEA can compete more efficiently with the peptide mimetic, the relatively high dissociation rate of 1.1×10^{-2} s^{-1} may lead to a loss of the signal generating labels during subsequent washing steps. Higher concentrations of the capture antibody and peptide mimetic would possibly lead to higher signals in ELISA and FIA. For practical reasons, however, this is not an option because higher antibody coating concentrations would drastically increase the assay costs, and higher concentrations of the peptide mimetic would decrease the sensitivity of the competitive immunoassay. Therefore, we replaced SA-FAM and SA-HRP by a UCNP-PEG-SA label to develop a robust method for the detection of ZEA in food samples. In addition to the background-free optical detection, each UCNP label exposes several streptavidin molecules on its surface connected via a highly flexible PEG-linker structure. We expected that the UCNP label with its ability to strongly bind to several peptides simultaneously via the biotin-streptavidin interaction (multivalency) would partially compensate for the relatively weak affinity of the peptide bound to the capture antibody.

3.5. Characterization of UCNP labels

Oleic acid-capped UCNPs ($NaYF_4$:Yb^{3+},Tm^{3+}) were modified with alkyne-PEG-neridronate ligand and streptavidin-azide (Fig. 1; bottom left inset) by a Cu-catalyzed click-reaction (Mickert et al., 2019; Farka et al., 2020b). The as-synthesized UCNPs and the UCNP-PEG-SA-bioconjugates were thoroughly characterized before employing them as a label in the competitive immunoassay. Transmission electron microscopy (TEM) revealed a uniform spherical shape (Fig. 4A) with an average diameter of 37 nm (Fig. 4B). In the emission spectrum (Fig. 4C), the UCNPs displayed the strongest luminescence at 800 nm. Moreover, the hydrodynamic properties of particles before and after the conjugation were compared by dynamic light scattering (DLS). The increase of the hydrodynamic diameter (Fig. 4D and E) indicated the successful surface modification of UCNPs. As the distribution of the hydrodynamic diameter did not broaden considerably, the conjugation procedure did not lead to particle aggregation. Finally, the functional properties of the conjugate were tested in a BSA-biotin assay (Fig. 4F). The UCNP-PEG-SA conjugate resulted in a S/B of 622 for 100 ng mL^{-1} of immobilized BSA-biotin and 35 μg mL^{-1} of UCNP-PEG-SA. At this BSA-biotin concentration, SA-HRP or SA-FAM achieved only a S/B of 4 or 7, respectively, which shows the superior performance of UCNP labels.

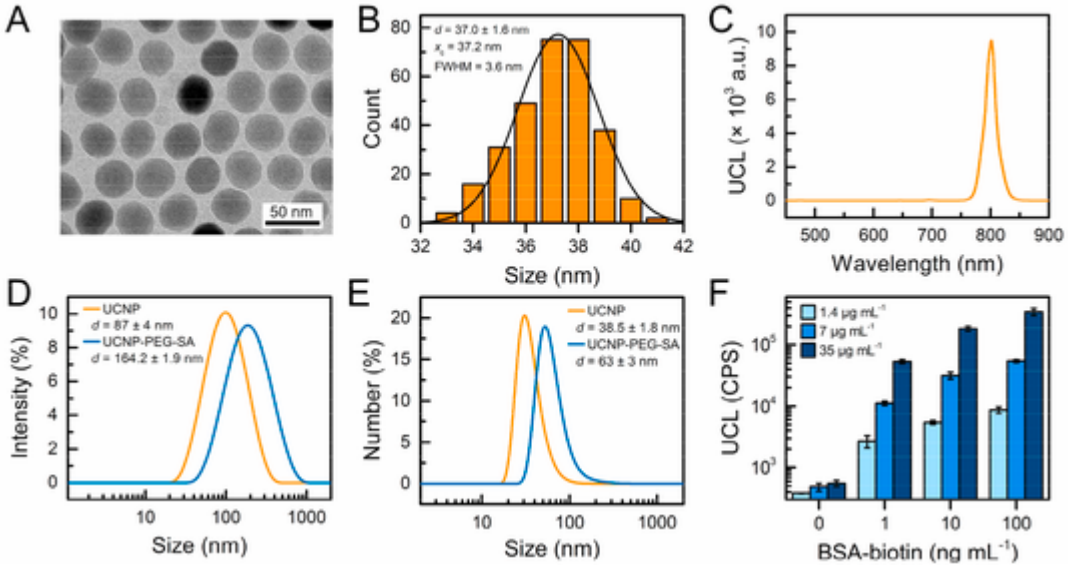

Fig. 4. Characterization of UCNPs. (A) TEM image of oleic-acid capped UCNPs. (B) Size distribution of UCNPs determined from TEM. (C) Emission spectrum of UCNPs measured under 980-nm excitation. DLS measurements (D: intensity; E: number distribution) of oleic acid-capped UCNPs in cyclohexane and UCNP-PEG-SA-conjugates in TBS. (F) Binding of UCNP-PEG-SA-conjugates (concentrations of 1.4–35 μg mL^{-1}) to immobilized BSA-biotin. The error bars show the standard error of the mean in replicate wells (n = 3).

3.6. Competitive upconversion-linked immunosorbent assay (ULISA)

The anti-ZEA capture antibody was immobilized onto a well of a microtiter plate, and the competition between ZEA and the biotinylated peptide mimetic was detected using the UCNP-PEG-SA label as shown in Fig. 1. The competitive ULISA was optimized in terms of the antibody and peptide concentrations, assay and blocking buffer, as well as the UCNP label concentration (Fig. S7). High concentrations of the capture antibody and peptide mimetic resulted in higher absolute signals in the absence of free ZEA (Fig. S7A). Lowering these concentrations improved the sensitivity towards ZEA detection. The optimal concentrations were high enough to provide reliable signals but also resulted in good sensitivity for the detection of ZEA. The effect of the assay buffer composition was also studied, but the tested buffers exerted only minor effects on the assay sensitivity (Fig. S7B). The assay buffer containing BGG and BSA-based blocking buffer was selected as it provided slightly better sensitivity to ZEA, albeit lower absolute signals compared to the SuperBlock-based buffer (Fig. S7B). The more complex BGG-containing assay buffer led to lower background signals, thus strongly improving the S/B to 45 compared to the SuperBlock-based buffer (S/B: 17). The same assay buffer composition was used previously in a highly sensitive ULISA for the detection of prostate-specific antigen (PSA) in serum (Mickert et al., 2019), and it is considered to be particularly suitable for complex samples and difficult matrices. Similarly, the assay performance was only marginally influenced by using either BSA or SuperBlock as the blocking buffer. However, the use of BSA resulted in a better S/B of 45 compared to SuperBlock (S/B 31), and it was selected for subsequent experiments. Higher UCNP concentrations provided higher absolute signals but did affect the sensitivity, and similar IC_{50} values of 0.19 (±0.03) ng mL^{-1} and 0.18 (±0.09) ng mL^{-1} were observed with 12.5 and 30 μg mL^{-1} UCNPs, respectively (Fig. S7C).

Fig. 5A shows the excellent performance of the optimized ULISA with an IC_{50} value of 0.16 ± 0.08 ng mL^{-1} and a dynamic range (IC_{20}–IC_{80}) from 50 pg mL^{-1} to 0.5 ng mL^{-1}. The LOD of 20 pg mL^{-1} was more than 200 times lower than our earlier bioluminescent immunoassay based on the same antibody and the same peptide mimetic sequence in the form of a fusion protein (Peltomaa et al., 2020). Also, the dynamic range was improved by a factor of 3 compared to the bioluminescent method. Overall, the LOD of the ULISA is comparable or lower than most of the previously reported methods (Table S1) and commercially available assays (Table S2). Although few lower LODs have been reported in the literature, the ULISA benefits from a simple and straightforward assay protocol and measurement scheme.

3.7. Cross-reactivity

The specificity of the ULISA was evaluated by determining the cross-reactivity with related mycotoxins. Metabolites of ZEA, such as the stereoisomers α-zearalenol and β-zearalenol, showed strong cross-reactivities of 320% and 133%, respectively (Fig. 5B) because they share a high structural similarity with ZEA (Fig. S8). Furthermore, the monoclonal anti-ZEA antibody was raised against an ovalbumin-ZEA conjugate, which consisted of ZEA attached to ovalbumin in the very position that is varied among these metabolites (Fig. S8). Thus, the antibody cannot differentiate between these metabolites in line with previous reports on antibodies raised against ZEA-oxime-coupled conjugates (Thouvenot and Morfin, 1983; Liu et al., 1985). In any case, cross-reactivity with these metabolites can be considered useful as both of them are *in vivo* metabolites of ZEA and have been shown to occur naturally (De Ruyck et al., 2020). Notably, no cross-reactivity was observed with other mycotoxins produced by the same *Fusarium* species (deoxynivalenol, ochratoxin A, fumonisin B_1, T-2 toxin).

3.8. Real sample analysis

We confirmed the functionality of the ULISA in a real sample matrix by spiking blank maize samples that were confirmed to be free of ZEA by UPLC-MS/MS analysis with 20–80 μg kg^{-1} of ZEA. Sample extracts in methanol were diluted in assay buffer and analyzed by the ULISA. Recoveries between 77% and 105% (Table 1) indicated an acceptable accuracy of the method for the quantitative detection of ZEA in real samples. The relative standard deviation (RSD) of three replicate measurements varied between 3 and 9%, thus also fulfilling the performance criteria for ZEA detection set in the European Commission regulations No 1881/2006 and 401/2006, which established a maximum residue limit of 350 μg kg^{-1} for unprocessed maize products and the acceptable recoveries and RSDs, respectively (European Commission, 2006a, 2014). The analysis of naturally contaminated maize samples

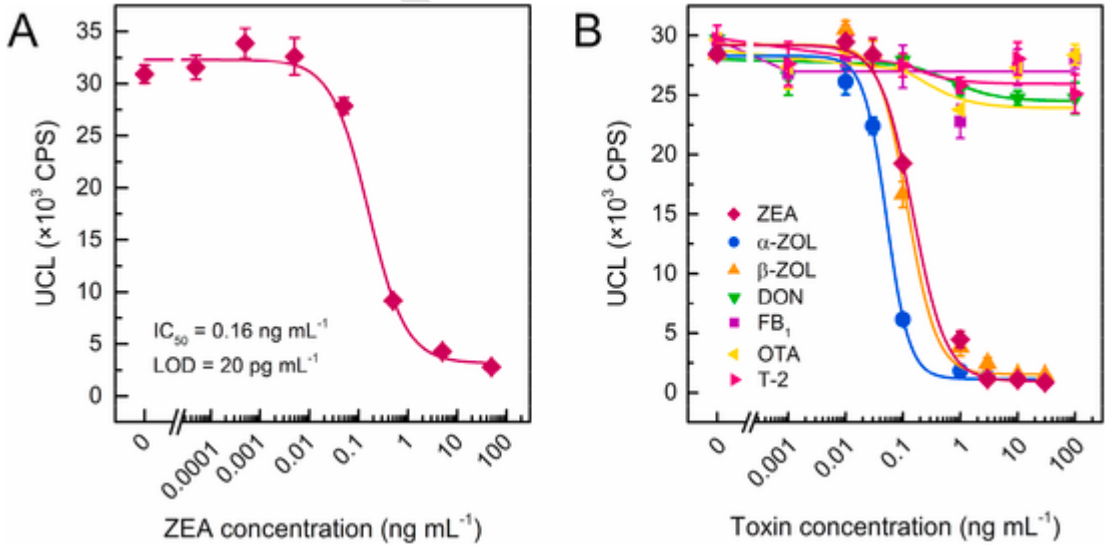

Fig. 5. (A) Calibration curve of the optimized ULISA for the detection of ZEA in buffer. (B) Cross-reactivities (CR) of zearalenone (ZEA, IC_{50}: 0.16 ± 0.08 ng ml^{-1}, CR: 100%); α-zearalenol (α-ZOL, IC_{50}: 0.05 ± 0.01 ng ml^{-1}, CR: 320%) and β-zearalenol (β- ZOL, IC_{50}: 0.12 ± 0.05 ng ml^{-1}, CR: 133%). No cross-reactivities (IC_{50} not determinable) are found for the toxins deoxynivalenol (DON), fumonisin B_1 (FB_1), ochratoxin A (OTA), and T-2 toxin (T-2). The molecular structures of the toxins are shown in Fig. S6. The error bars the standard error of the mean in replicate wells (n = 3).

Table 1
ULISA analysis of spiked samples (top) and naturally contaminated samples (bottom).

Spiked ZEA (μg kg $^{-1}$)	Measured ZEA (μg kg $^{-1}$)	RSD [a]	Recovery
0	< LOD	6%	*n.d.*
20	18.3	4%	91%
40	41.8	3%	105%
60	61.2	4%	102%
80	61.3	9%	77%
Measured ZEA (μg kg $^{-1}$) by UPLC-MS/MS	**Measured ZEA (μg kg $^{-1}$) by ULISA**	**RSD [a] of ULISA**	**Measured ZEA (μg kg $^{-1}$) by UPLC-MS/MS**
70	88	6%	70
114	108	12%	114
124	151	6%	124
250	184	4%	250
350	334	17%	350

[a] *RSD, relative standard deviation* (n = 3).

by both the competitive ULISA and UPLC-MS/MS yielded in general consistent results (Table 1). Depending on the type of sample, however, significant variations were observable between these methods that can be explained by matrix effects affecting the UPLC-MS/MS and ULISA measurement to a different degree. The stronger matrix effect in naturally contaminated samples is also evident from larger RSD values of the ULISA compared to the spiked samples. Despite these variations, the ULISA readily enables detection of ZEA concentration above maximum residue limits in naturally contaminated cereal samples.

4. Conclusions

We have demonstrated the advantages of using peptide mimetics in a competitive ULISA for the sensitive detection of the mycotoxin ZEA. The design of the competitive ULISA rests on two interdependent pillars: (1) A biotinylated peptide mimetic serves as a substitute for the conventional ZEA-protein conjugate that competes efficiently with the analyte ZEA as shown by NMR and SPR analyses of the peptide–antibody interaction. (2) A UCNP-PEG-SA conjugate serves as a substitute for the conventional enzyme label that attaches the label more strongly and can be detected without optical background interference. With an LOD of 20 pg mL^{-1} (63 pM), is about 1000 × more sensitive than commercial assays for ZEA detection. Furthermore, no complex sample pre-treatment is required as for common reference methods such as HPLC-MS. The method also showed good analytical performance not only in buffer but also in spiked and naturally contaminated maize samples. Therefore, our competitive ULISA is a valuable tool for the simple analysis of mycotoxin-contaminated food samples with a sensitivity that meets the requirements set by the European legislation.

Declaration of competing interest

The authors declare that they have no known competing financial interests or personal relationships that could have appeared to influence the work reported in this paper.

Acknowledgements

This study was supported by the German Research Foundation (DFG: GO 1968/5–1) and the Spanish Ministry of Science, Innovation and Universities (projects RTI2018-096410-B-C21, PID2019-1052376 B-I00, CTQ2016-76263-P, and a FPI fellowship for M.M.O.). R.P. acknowledges Universidad Complutense de Madrid (UCM) for a research grant and H. H. G. the DFG for support within the Heisenberg Program (GO 1968/7–1). Z.F., M.P., and P.S. acknowledge financial support from the Ministry of Education, Youth and Sports of the Czech Republic (MEYS CR) under the projects CEITEC 2020 (LQ1601) and INTER-ACTION (LTAB19011). A.H. acknowledges support from Czech Science Foundation (18-03367Y) and Institutional support RVO 68081715 of the Institute of Analytical Chemistry, Czech Academy of Sciences. We thank Vít Vykoukal for taking TEM images and Thomas Hirsch for providing the equipment for DLS measurements. CI-ISB research infrastructure project LM2018127 funded by MEYS CR is acknowledged for the financial support of the measurements at the CF Cryo-electron Microscopy and Tomography, and CF Nanobiotechnology.

Appendix A. Supplementary data

Supplementary data to this article can be found online at https://doi.org/10.1016/j.bios.2020.112683.

References

Bennett, J.W., Klich, M., 2003. Mycotoxins. Clin. Microbiol. Rev. 16, 497–516.
Caglayan, M.O., Şahin, S., Üstündağ, Z., 2020. Detection strategies of zearalenone for food safety: a review. Crit. Rev. Anal. Chem. 26, 1–20.
Chauhan, R., Singh, J., Sachdev, T., Basu, T., Malhotra, B.D., 2016. Recent advances in mycotoxins detection. Biosens. Bioelectron. 81, 532–545.
Dai, S., Wu, S., Duan, N., Chen, J., Zheng, Z., Wang, Z., 2017. An ultrasensitive aptasensor for Ochratoxin A using hexagonal core/shell upconversion nanoparticles as luminophores. Biosens. Bioelectron. 91, 538–544.
De Ruyck, K., Huybrechts, I., Yang, S., Arcella, D., Claeys, L., Abbeddou, S., De Keyzer, W., De Vries, J., Ocke, M., Ruprich, J., De Boevre, M., De Saeger, S., 2020. Mycotoxin exposure assessments in a multi-center European validation study by 24-hour dietary recall and biological fluid sampling. Environ. Int. 137, 105539.
De Saeger, S., Sibanda, L., Van Peteghem, C., 2003. Analysis of zearalenone and α-zearalenol in animal feed using high-performance liquid chromatography. Anal. Chim. Acta 487, 137–143.
Drzymala, S.S., Weiz, S., Heinze, J., Marten, S., Prinz, C., Zimathies, A., Garbe, L.-A., Koch, M., 2015. Automated solid-phase extraction coupled online with HPLC-FLD for the quantification of zearalenone in edible oil. Anal. Bioanal. Chem. 407, 3489–3497.
EFSA Panel on Contaminants in the Food Chain (CONTAM), 2011. Scientific Opinion on the risks for public and animal health related to the presence of zearalenone in food. EFSA Journal 2011, 2197.
European Commission, 2006. Commission regulation (EC) No 1881/2006. Off. J. Eur. Union L364, 5–24.
European Commission, 2006. Commission recommendation (EC) No 576/2006. Off. J. Eur. Union L229, 7–9.
European Commission, 2014. Commission regulation (EC) No 519/2014. Off. J. Eur. Union L147, 29–43.
European Commission Opinion of the scientific committee on food on *Fusarium* toxins. Part 2: zearalenone (ZEA)Available at:https://ec.europa.eu/food/sites/food/files/safety/docs/cs_contaminants_catalogue_fusarium_out65_en.pdf2000
Fang, G., Fan, C., Liu, H., Pan, M., Zhu, H., Wang, S., 2014. A novel molecularly imprinted polymer on CdSe/ZnS quantum dots for highly selective optosensing of mycotoxin zearalenone in cereal samples. RSC Adv. 4, 2764–2771.
Farka, Z., Juřík, T., Kovář, D., Trnková, L., Skládal, P., 2017. Nanoparticle-based immunochemical biosensors and assays: recent advances and challenges. Chem. Rev. 117, 9973–10042.
Farka, Z., Mickert, M.J., Mikušová, Z., Hlaváček, A., Bouchalová, P., Xu, W., Bouchal, P., Skládal, P., Gorris, H.H., 2020. Surface design of photon-upconversion nanoparticles for high-contrast immunocytochemistry. Nanoscale 12, 8303–8313.
Farka, Z., Mickert, M.J., Pastucha, M., Mikušová, Z., Skládal, P., Gorris, H.H., 2020. Advances in optical single-molecule detection: en route to supersensitive bioaffinity assays. Angew. Chem. Int. Ed. 59, 10746–10773.
M. Gareis R.C. Schothorst A. Vidnes C. Bergsten B. Paulsen C. Brera M. Miraglia Collection of occurrence data of Fusarium toxins in food and assessment of dietary intake by the population of EU Member States. Report of Experts Participating in SCOOP Task 3.2.10available at:https://ec.europa.eu/food/sites/food/files/safety/docs/cs_contaminants_catalogue_fusarium_task3210.pdf2003
Haase, M., Schäfer, H., 2011. Upconverting nanoparticles. Angew. Chem. Int. Ed. 50, 5808–5829.
Hlaváček, A., Farka, F., Hübner, M., Horňáková, V., Němeček, D., Niessner, R., Skládal, P., Knopp, D., Gorris, H.H., 2016. Competitive upconversion-linked immunosorbent assay for the sensitive detection of diclofenac. Anal. Chem. 88, 6011–6017.
He, D., Wu, Z., Cui, B., Jin, Z., Xu, E., 2020. A fluorometric method for aptamer-based simultaneous determination of two kinds of the *Fusarium* mycotoxins zearalenone and fumonisin B_1 making use of gold nanorods and upconversion nanoparticles. Microchim. Acta 187, 254.
He, Q.-H., Xu, Y., Huang, Y.-H., Liu, R.-R., Huang, Z.-B., Li, Y.-P., 2011. Phage-displayed peptides that mimic zearalenone and its application in immunoassay. Food Chem. 126, 1312–1315.

He, Z., He, Q., Xu, Y., Li, Y., Liu, X., Chen, B., Lei, D., Sun, C., 2013. Ochratoxin A mimotope from second-generation peptide library and its application in immunoassay. Anal. Chem. 85, 10304–10311.

Hidalgo-Ruiz, J.L., Romero-González, R., Martínez Vidal, J.L., Garrido Frenich, A., 2019. A rapid method for the determination of mycotoxins in edible vegetable oils by ultra-high performance liquid chromatography-tandem mass spectrometry. Food Chem. 288, 22–28.

IARC, International Agency for Research on Cancer, 1993. Monographs on the Evaluation of Carcinogenic Risks to Humans, Some Naturally Occurring Substances: Food Items and Constituents, Heterocyclic Aromatic Amines and Mycotoxins. International Agency for Research on Cancer, Lyon, France.

Jiang, F., Li, P., Zong, C., Yang, H., 2020. Surface-plasmon-coupled chemiluminescence amplification of silver nanoparticles modified immunosensor for high-throughput ultrasensitive detection of multiple mycotoxins. Anal. Chim. Acta 1114, 58–65.

Kim, K., Jo, E.-J., Lee, K.J., Park, J., Jung, G.Y., Shin, Y.-B., Lee, L.P., Kim, M.-G., 2020. Gold nanocap-supported upconversion nanoparticles for fabrication of a solid-phase aptasensor to detect ochratoxin. A. Biosens. Bioelectron. 150, 111885.

Kuiper-Goodman, T., Scott, P.M., Watanabe, H., 1987. Risk assessment of the mycotoxin zearalenone. Regul. Toxicol. Pharmacol. 7, 253–306.

Li, R., Meng, C., Wen, Y., Fu, W., He, P., 2019. Fluorometric lateral flow immunoassay for simultaneous determination of three mycotoxins (aflatoxin B_1, zearalenone and deoxynivalenol) using quantum dot microbeads. Microchim. Acta 186, 748.

Liu, M.-T., Ram, B.P., Hart, L.P., Pestka, J.J., 1985. Indirect enzyme-linked immunosorbent assay for the mycotoxin zearalenone. Appl. Environ. Microbiol. 50, 5.

Liu, X., Xu, Y., He, Q., He, Z., Xiong, Z., 2013. Application of mimotope peptides of fumonisin B_1 in peptide ELISA. J. Agric. Food Chem. 61, 4765–4770.

Liu, Z., Hua, Q., Wang, J., Liang, Z., Li, J., Wu, J., Shen, X., Lei, H., Li, X., 2020. A smartphone-based dual detection mode device integrated with two lateral flow immunoassays for multiplex mycotoxins in cereals. Biosens. Bioelectron. 158, 112178.

Maaroufi, K., Chekir, L., Creppy, E.E., Ellouz, F., Bacha, H., 1996. Zearalenone induces modifications of haematological and biochemical parameters in rats. Toxicon 34, 535–540.

Magnusson, B., Örnemark, U. (Eds.), 2014. Eurachem Guide: the Fitness for Purpose of Analytical Methods – A Laboratory Guide to Method Validation and Related Topics, second ed. Available at:. http://www.eurachem.org.

Marco, M.-P., Gee, S., Hammock, B.D., 1995. Immunochemical techniques for environmental analysis I. Immunosensors. Trends Anal. Chem. 14, 341–350.

Mayer, M., Meyer, B., 1999. Characterization of ligand binding by saturation transfer difference NMR spectroscopy. Angew. Chem. Int. Ed. 38, 1784–1788.

Mickert, M.J., Farka, Z., Kostiv, U., Hlaváček, A., Horák, D., Skládal, P., Gorris, H.H., 2019. Measurement of sub-femtomolar concentrations of prostate-specific antigen through single-molecule counting with an upconversion-linked immunosorbent assay. Anal. Chem. 91, 9435–9441.

Niazi, S., Wang, X., Pasha, I., Khan, I.M., Zhao, S., Shoaib, M., Wu, S., Wang, Z., 2018. A novel bioassay based on aptamer-functionalized magnetic nanoparticle for the detection of zearalenone using time resolved-fluorescence $NaYF_4$: Ce/Tb nanoparticles as signal probe. Talanta 186, 97–103.

Nolan, P., Auer, S., Spehar, A., Elliott, C.T., Campbell, K., 2019. Current trends in rapid tests for mycotoxins. Food Addit. Contam. A 36, 800–814.

Peltomaa, R., Agudo-Maestro, I., Más, V., Barderas, R., Benito-Peña, E., Moreno-Bondi, M.C., 2019. Development and comparison of mimotope-based immunoassays for the analysis of fumonisin B_1. Anal. Bioanal. Chem. 411, 6801–6811.

Peltomaa, R., Amaro-Torres, F., Carrasco, S., Orellana, G., Benito-Peña, E., Moreno-Bondi, M.C., 2018. Homogeneous quenching immunoassay for fumonisin B_1 based on gold nanoparticles and an epitope-mimicking yellow fluorescent Protein. ACS Nano 12, 11333–11342.

Peltomaa, R., Benito-Peña, E., Barderas, R., Sauer, U., González Andrade, M., Moreno-Bondi, M.C., 2017. Microarray-based immunoassay with synthetic mimotopes for the detection of fumonisin B_1. Anal. Chem. 89, 6216–6223.

Peltomaa, R., Benito-Peña, E., Moreno-Bondi, M.C., 2018. Bioinspired recognition elements for mycotoxin sensors. Anal. Bioanal. Chem. 410, 747–771.

Peltomaa, R., Fikacek, S., Benito-Peña, E., Barderas, R., Head, T., Deo, S., Daunert, S., Moreno-Bondi, M.C., 2020. Bioluminescent detection of zearalenone using recombinant peptidomimetic *Gaussia* luciferase fusion protein. Microchim Acta 187, 547.

Romera, D., Mateo, E.M., Mateo-Castro, R., Gómez, J.V., Gimeno-Adelantado, J.V., Jiménez, M., 2018. Determination of multiple mycotoxins in feedstuffs by combined use of UPLC–MS/MS and UPLC–QTOF–MS. Food Chem. 267, 140–148.

Sedlmeier, A., Hlaváček, A., Birner, L., Mickert, M.J., Muhr, V., Hirsch, T., Corstjens, P.L.A.M., Tanke, H.J., Soukka, T., Gorris, H.H., 2016. Highly sensitive laser scanning of photon-upconverting nanoparticles on a macroscopic scale. Anal. Chem. 88, 1835–1841.

Taghdisi, S.M., Danesh, N.M., Beheshti, H.R., Ramezani, M., Abnous, K., 2016. A novel fluorescent aptasensor based on gold and silica nanoparticles for the ultrasensitive detection of ochratoxin A. Nanoscale 8, 3439–3446.

Tan, H., Ma, L., Guo, T., Zhou, H., Chen, L., Zhang, Y., Dai, H., Yu, Y., 2019. A novel fluorescence aptasensor based on mesoporous silica nanoparticles for selective and sensitive detection of aflatoxin B_1. Anal. Chim. Acta 1068, 87–95.

Thouvenot, D., Morfin, R.F., 1983. Radioimmunoassay for zearalenone and zearalanol in human serum: production, properties, and use of porcine antibodies. Appl. Environ. Microbiol. 45, 16–23.

van Egmond, H.P., Schothorst, R.C., Jonker, M.A., 2007. Regulations relating to mycotoxins in food: perspectives in a global and European context. Anal. Bioanal. Chem. 389, 147–157.

Wild, D. (Ed.), 2013. The Immunoassay Handbook: Theory and Applications of Ligand Binding, ELISA, and Related Techniques, fourth ed. Elsevier, Oxford ; Waltham, MA.

Wu, S., Liu, L., Duan, N., Wang, W., Yu, Q., Wang, Z., 2018. A test strip for ochratoxin A based on the use of aptamer-modified fluorescence upconversion nanoparticles. Microchim. Acta 185, 497.

Xiong, Ying, Leng, Y., Li, X., Huang, X., Xiong, Yonghua, 2020. Emerging strategies to enhance the sensitivity of competitive ELISA for detection of chemical contaminants in food samples. Trends Anal. Chem. 126, 115861.

Yang, M., Zhang, Y., Cui, M., Tian, Y., Zhang, S., Peng, K., Xu, H., Liao, Z., Wang, H., Chang, J., 2018. A smartphone quantitative detection platform of mycotoxins based on multiple-color upconversion nanoparticles. Nanoscale 10, 15865–15874.

Yuan, Q., Pestka, J.J., Hespenheide, B.M., Kuhn, L.A., Linz, J.E., Hart, L.P., 1999. Identification of mimotope peptides which bind to the mycotoxin deoxynivalenol-specific monoclonal antibody. Appl. Environ. Microbiol. 65, 8.

Zhang, S., Sun, Y., Sun, Y., Wang, H., Shen, Y., 2020. Semiquantitative immunochromatographic colorimetric biosensor for the detection of dexamethasone based on up-conversion fluorescent nanoparticles. Microchim. Acta. 187, 447.

Zhang, Z., Shikha, S., Liu, J., Zhang, J., Mei, Q., Zhang, Y., 2019. Upconversion nanoprobes: recent advances in sensing applications. Anal. Chem. 91, 548–568.

Zinedine, A., Soriano, J.M., Moltó, J.C., Mañes, J., 2007. Review on the toxicity, occurrence, metabolism, detoxification, regulations and intake of zearalenone: an oestrogenic mycotoxin. Food Chem. Toxicol. 45, 1–18.